Electronic Supplementary Information for:

Origin of Pressure-Induced Band Gap Tuning in Tin Halide Perovskites

Mauro Coduri,[a] Thomas B. Shiell,[b] Timothy A. Strobel,[b] Arup Mahata,[c,d] Federico Cova,[e] Edoardo Mosconi,[d] Filippo De Angelis,[c,d,f,g*] and Lorenzo Malavasi[a,*]*

[a] Department of Chemistry and INSTM, Viale Taramelli 16, 27100, Pavia, Italy

[b]Earth and Planets Laboratory, Carnegie Institution for Science, Washington, DC 20015, USA

[c] CompuNet, Istituto Italiano di Tecnologia, Via Morego 30, 16163 Genova, Italy.

[d] Computational Laboratory for Hybrid/Organic Photovoltaics (CLHYO), CNR-SCITEC, via Elce di Sotto 8, I-06123 Perugia, Italy

[e] ESRF – The European Synchrotron, 81, Avenue des Martyrs, 38000, Grenoble, France.

[f] Department of Chemistry, Biology and Biotechnology, University of Perugia, Via Elce di Sotto 8, 06123 Perugia, Italy.

[g] Chemistry Department, College of Science, King Saud University, Riyadh, Saudi Arabia.

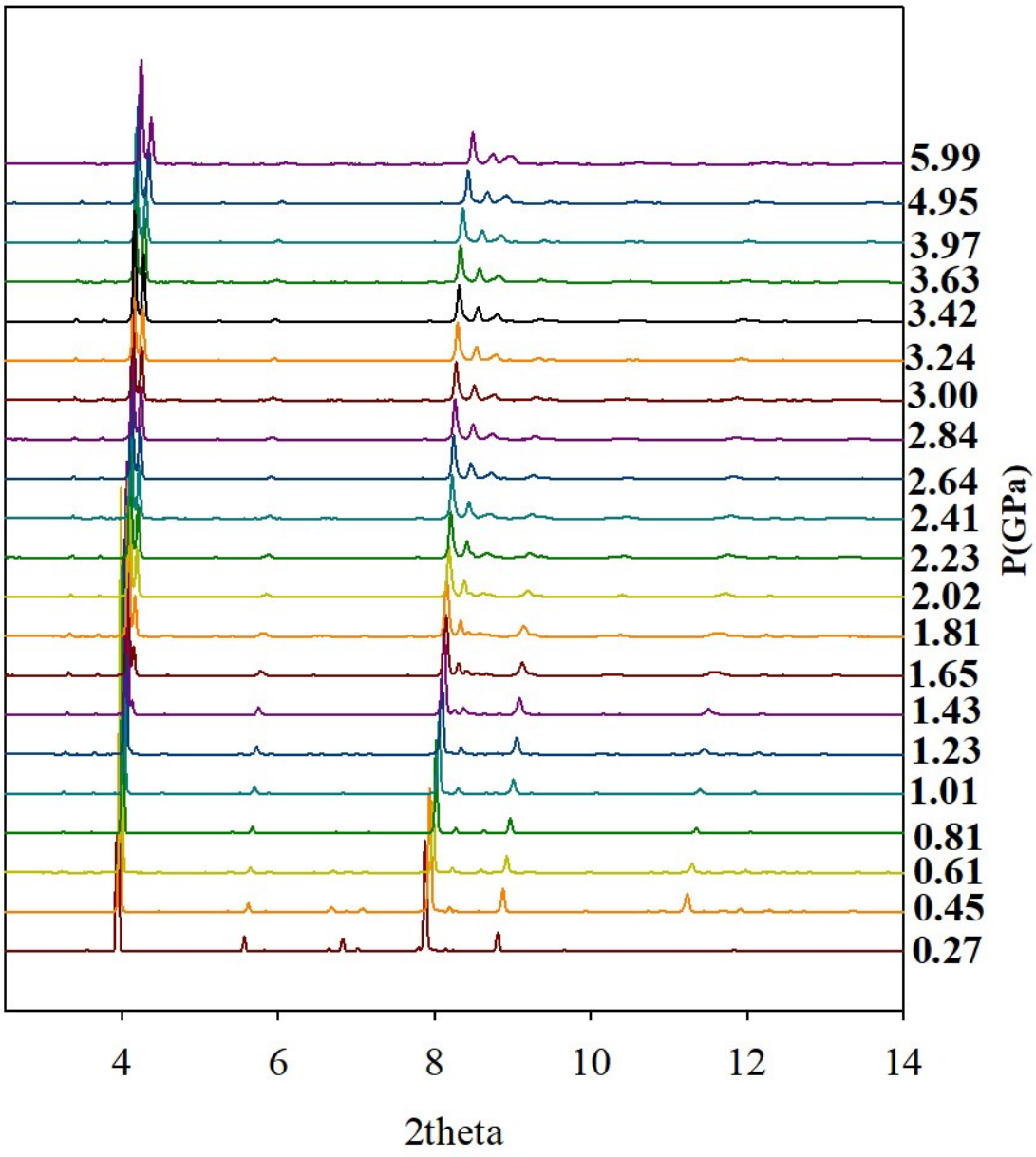

Figure S1: Integrated patterns of $FASnBr_3$ for all experimental pressure points upon increasing pressure.

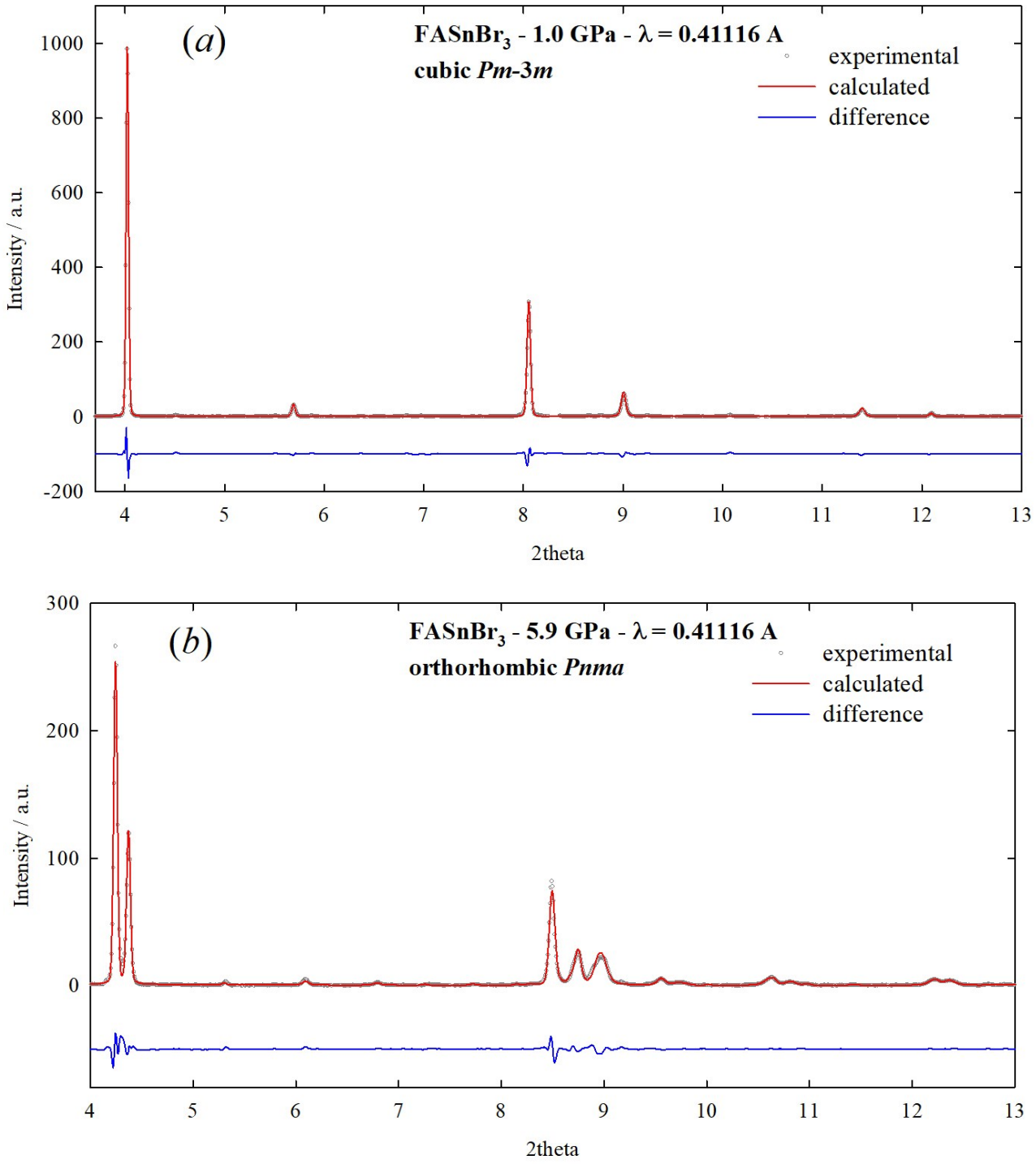

Figure S2: XRD refinements of $FASnBr_3$ with the cubic phase at 1.0 GPa (a) and with the orthorhombic phase at 5.9 GPa (b).

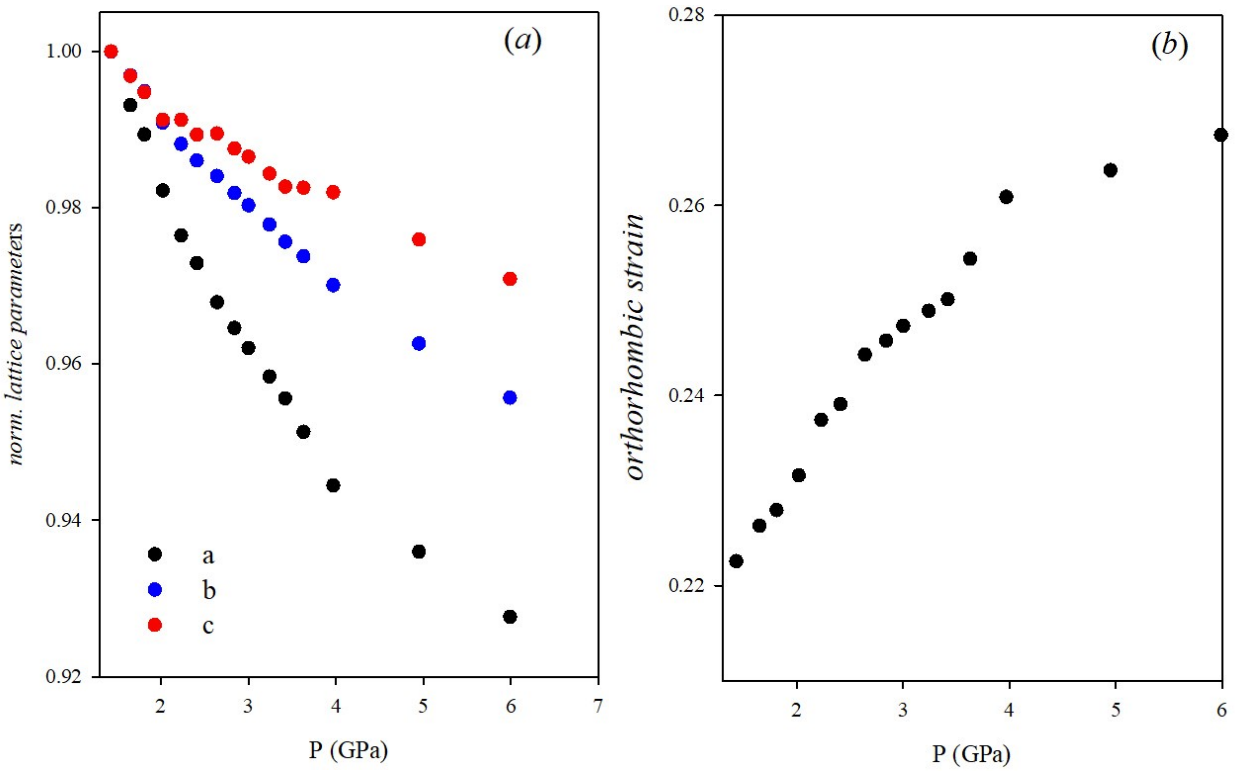

Figure S3: (*a*) Lattice parameters normalized against the values obtained at 1.43 GPa, *i.e.* the first pressure point where the structure is found orthorhombic. (*b*) Orthorhombic strain, defined as 2(a-b)/(a+b), as a function of pressure.

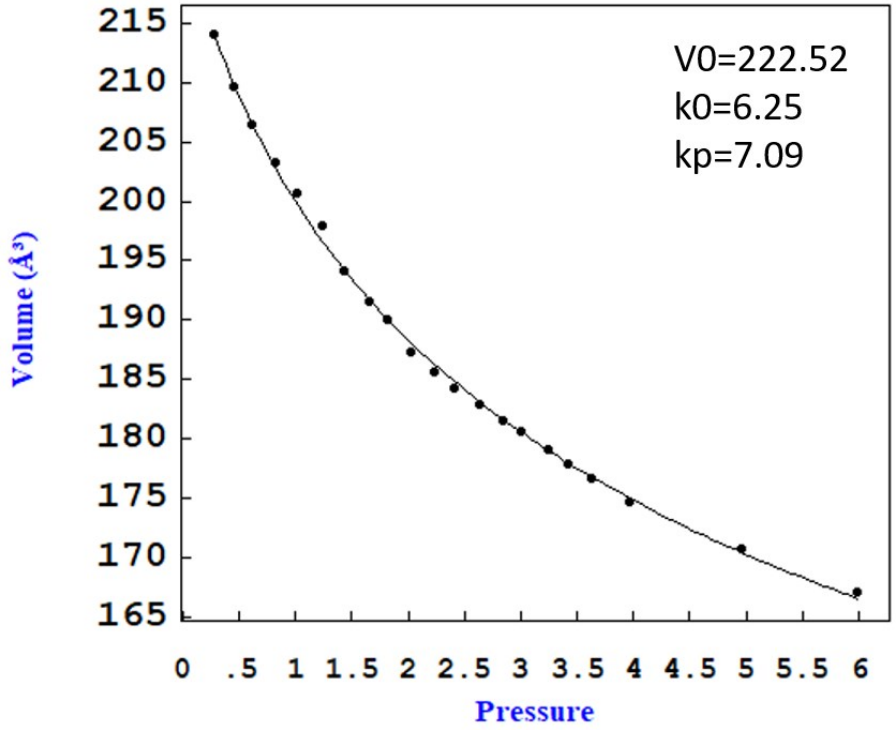

Figure S4: Fit of the volume as a function of pressure using the software EosFit7-GUI (S1) applying the Murnagham equation of state: $V_{PT} = V_{0T}\left(1 + \frac{K'_{0T}P}{K_{0T}}\right)^{-1}$. Refined parameters are given in the figure.

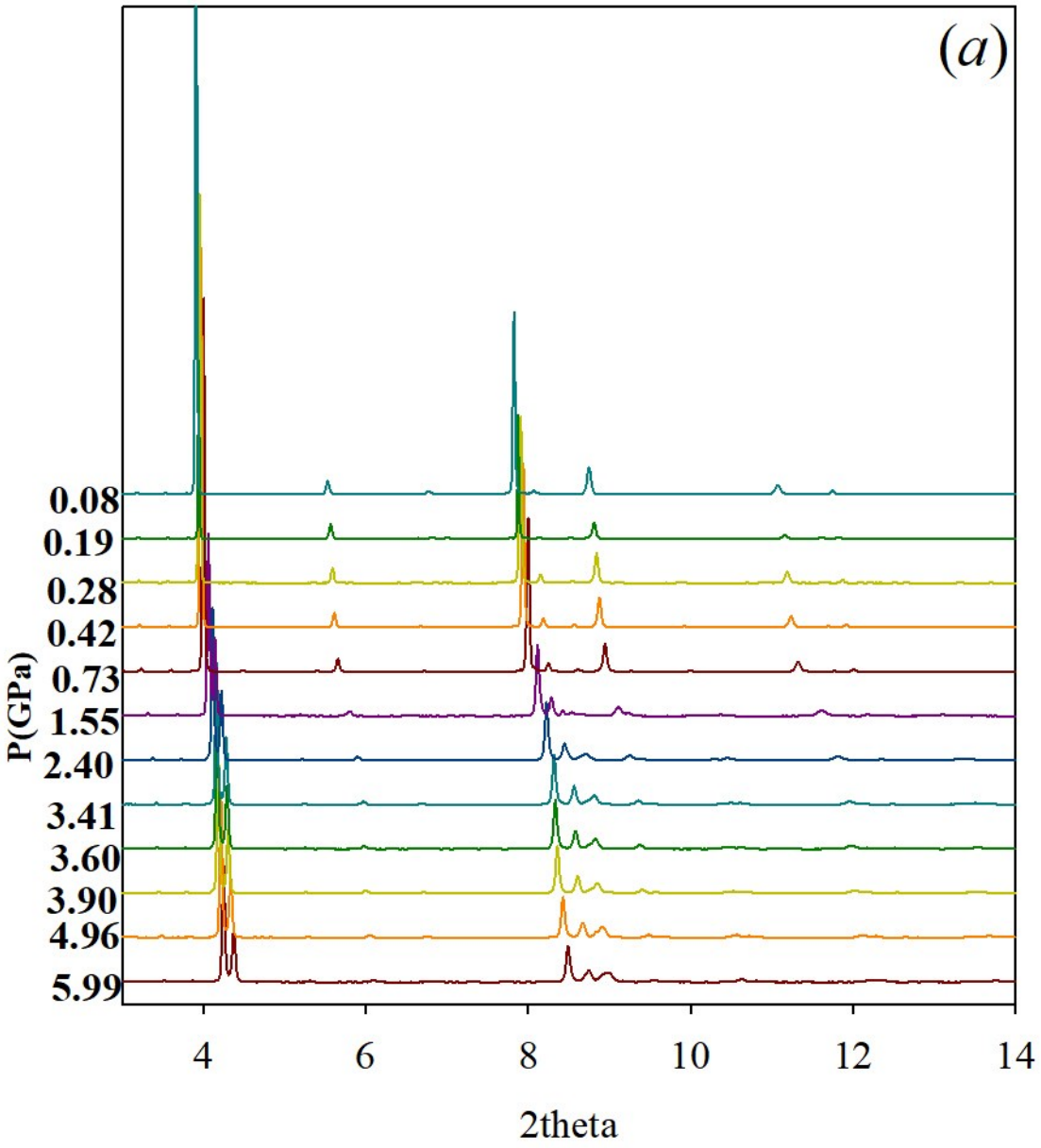

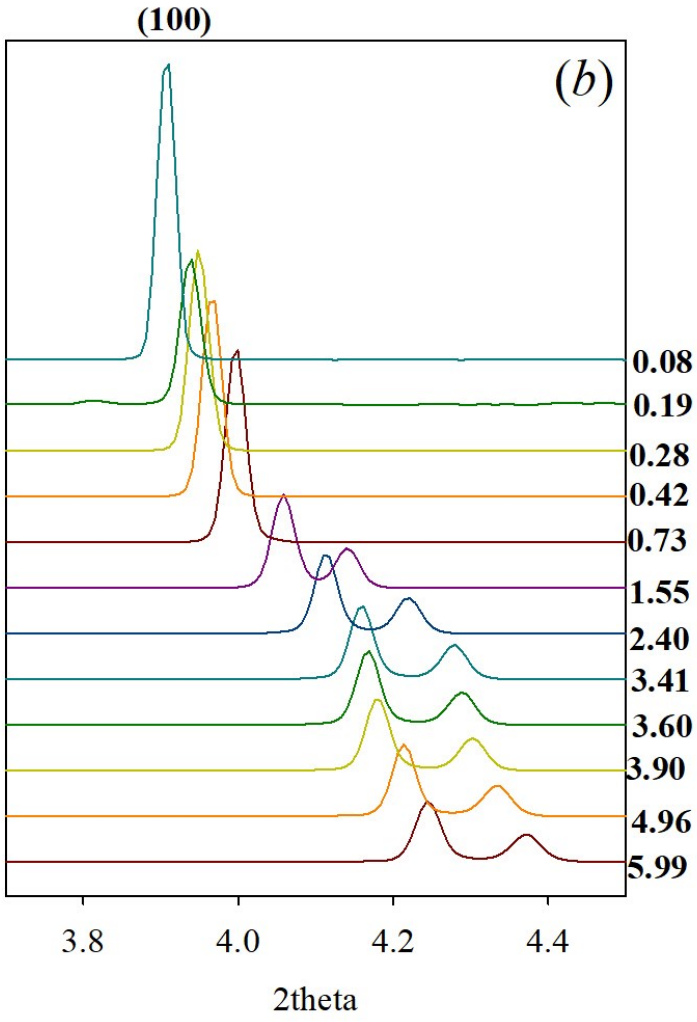

Figure S5: (a) Integrated patterns of $FASnBr_3$ for all experimental pressure points upon decreasing pressure; (b) same data in a smaller 2theta region to highlight the main peaks.

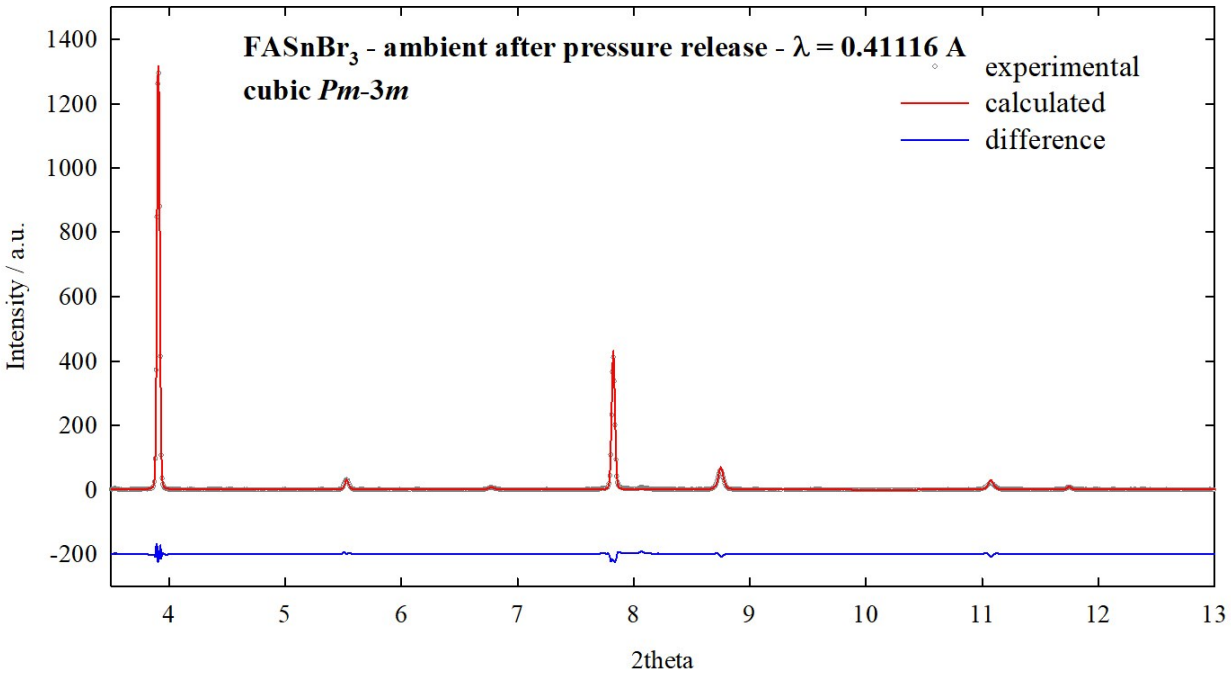

Figure S6: Cubic refined structures for $FASnBr_3$ after pressure release.

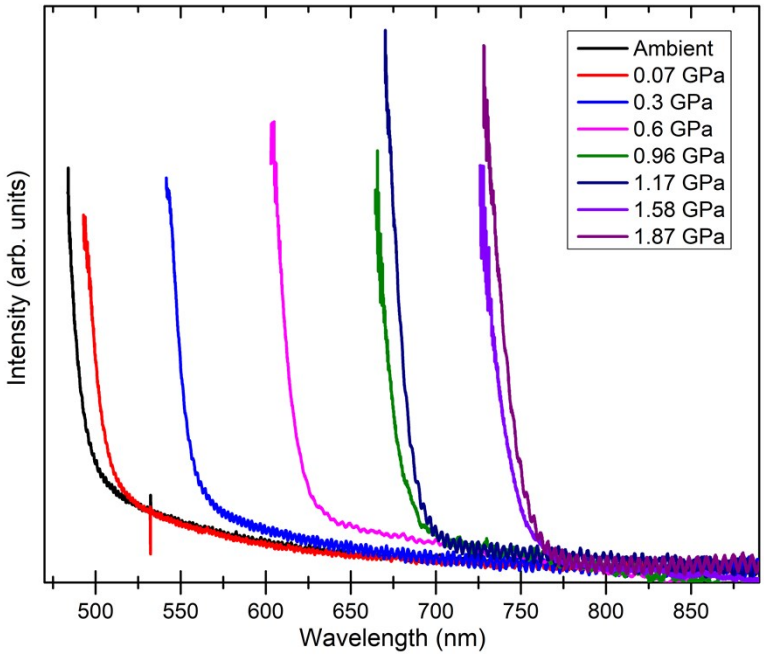

Figure S7: Optical absorption spectra of $FASnBr_3$ under pressure from ambient up to 1.87 GPa.

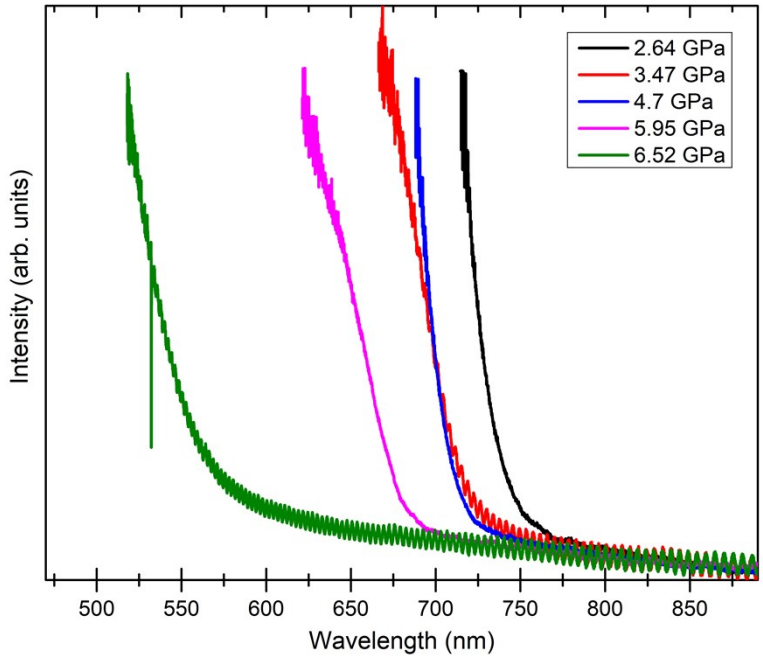

Figure S8: Optical absorption spectra of $FASnBr_3$ under pressure from 2.64 GPa up to 6.52 GPa.

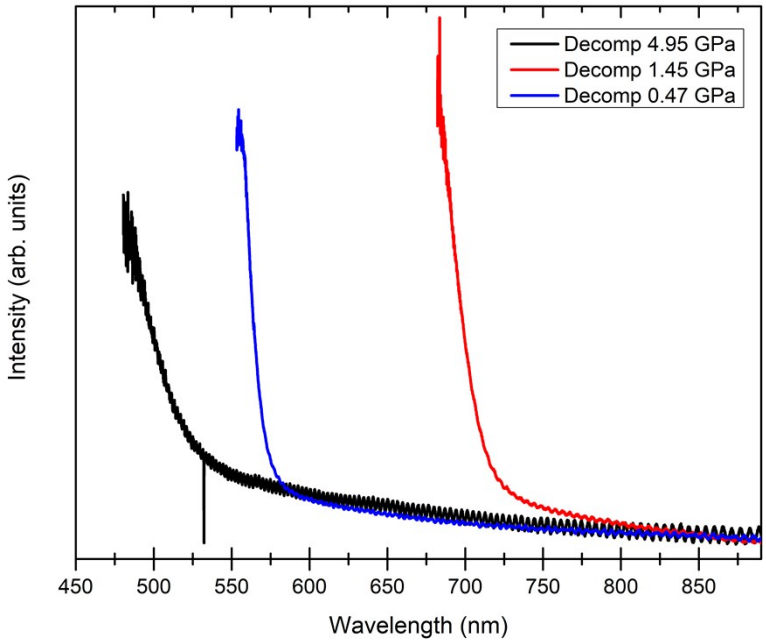

Figure S9: Optical absorption spectra of $FASnBr_3$ on decompression from 4.95 GPa up to 0.47 GPa.

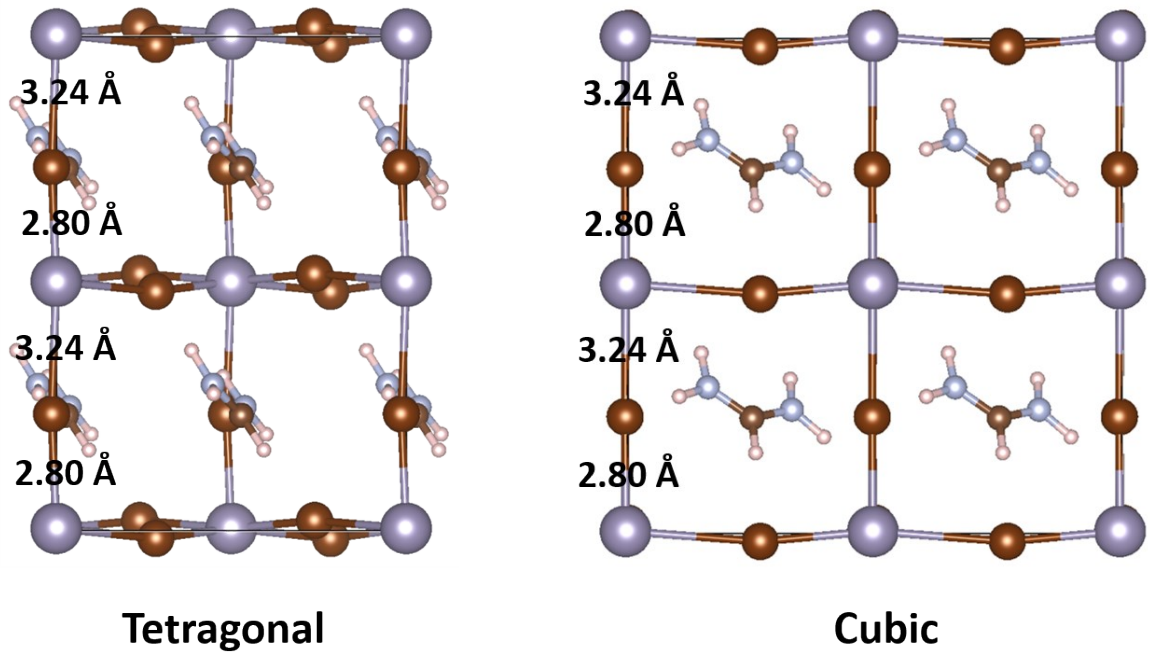

Figure S10: Optimized structural properties of tetragonal and cubic lattice.

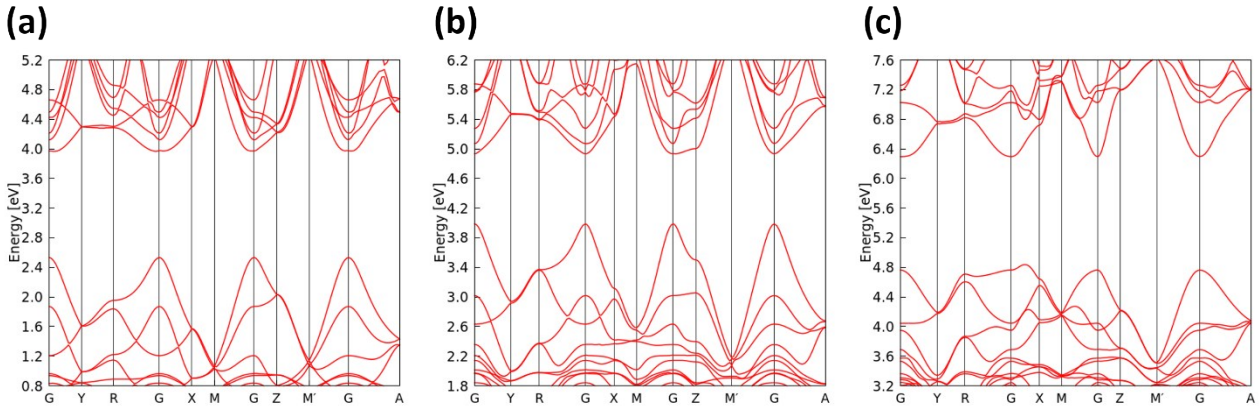

Figure S11: Electronic band structure of $FASNBr_3$ calculated by GGA-PBE level of theory under (a) ambient, (b) 1.65 GPa and (c) 5.99 GPa pressure. The high symmetry points across the Brillouin zone are G (0.0, 0.0, 0.0); Y (0.0, 0.5, 0.0); R (0.5, 0.5, 0.0); X (0.5, 0.0, 0.0); M (0.5, 0.0, 0.5); Z (0.0, 0.0, 0.5); M` (0.0, 0.5, 0.5) and A (0.5, 0.5, 0.5).

Text S1. Computational methods

Computational methods:

First-principles calculations based on density functional theory (DFT) are carried out as implemented in the PWSCF Quantum-Espresso package.[S2] Geometry optimization is performed using GGA-PBE[S3] level of theory and the electrons-ions interactions were described by ultrasoft pseudo-potentials with electrons from Br 4s, 4p; N, C 2s, 2p; H 1s; Sn 5s, 5p, 4d; shells explicitly included in calculations. Electronic structure are calculated by a single point hybrid calculations including SOC using the modified version of the HSE06 functional[S4] including 43% Hartree-Fock exchange proposed in Ref.[S5] with norm-conserving pseudo potentials with electrons from Br 4s, 4p; N, C 2s, 2p; H 1s; Sn 4s, 4p, 5s, 5p, 4d; shells explicitly included in calculations.

The experimental cell parameters have been used in all the cases. We have considered tetragonal lattice by rotating the cubic lattice parameters under ambient pressure for better comparison of structural and electronic properties with the high pressure orthorhombic structure. Geometry optimizations for 2×2×1 tetragonal/orthorhombic supercell (48 atoms) are performed with a k-point sampling[S6] of 4×4×2 along with plane-wave basis set cutoffs for the smooth part of the wave functions and augmented electronic density expansions of 25 and 200Ry, respectively. HSE06-SOC calculation have been performed 2×2×2 k-point sampling with plane-wave basis set cutoffs for the smooth part of the wave functions and augmented electronic density expansions of 40 and 80Ry, respectively. For the cubic structure, 2×2×2 k-point sampling has been used for geometry optimization.

Text S2. Experimental Methods

Synthesis

$FASnBr_3$, a proper amount of Sn acetate is dissolved in an excess of HBr under nitrogen atmosphere and stirring. The solution is heated to 100 °C, and the formamidine is added in the required molar amounts, together with 3 mL of hypophosphorous acid. A precipitate is formed immediately after the amine addition. The solution is then slowly cooled down to 60 °C, then the precipitate is immediately filtered and dried under vacuum overnight.

Diamond anvil cell loading procedure for optical measurements

The $FASnBr_3$ powder was pumped into an Ar glove box (H_2O and O_2 < 0.5 ppm) for loading into diamond anvil cells. A small scoop of powder was placed between 1 mm culets and pressed together to make a thin pellet (roughly 10 microns thick). This pellet was then cut into a plate (~60×60 μm^2) and loaded into a diamond anvil cell. Two cells were used. The first utilized 400 μm culets and a ~60 μm thick Re gasket with 225 μm hole. The second utilized 600 μm culets with 90 μm thick Re gasket and 325 μm hole. All diamonds were type Ia and the 600 μm pair showed lower intrinsic fluorescence

with visible light excitation. After the pellet was transferred into the gasket hole, the gasket was sealed in the Ar glovebox (1atm) and the cell was removed. Measurements were taken at 1 atm before gas loading. High-pressure Ar was loaded into the cell using a gas loading apparatus at ~70 MPa after which the cell was sealed and removed for experiments. Each cell had large regions of Ar, which served as both the pressure transmitting medium and the reference region for optical measurements.

NIR/VIS transmission measurements

NIR/VIS absorbance was measured using a Bruker Vertex-70 spectrometer with a Hyperion microscope in transmission mode. A water-cooled NIR halogen lamp aligned to the back entry port of the instrument was passed to the sample through a quartz beam splitter. The light was focused on and collected through the sample using reflecting objectives and two sets of opaque slits before and after light collection were used to collimate light at approximately $50\times50\mu m^2$ before it was passed to a silicon diode detector. Transmission through the sample was measured as a function of pressure and transmission though the Ar served as the absorbance reference for each measurement.

NIR/VIS transmission was also measured using a homemade setup consisting a halogen light source (Mikropack DH-2000) and spectrograph. Light was passed through an optical fiber and focused on the sample using a 20× Mitutoyo objective lens after spatial collimation through a 50 μm pinhole. Transmitted light was collected by a second 20x Mitutoyo objective, passed through a 50 μm confocal pinhole and then focused on the entrance slit of a spectrograph (Princeton Instruments) with CCD detector. A reference spectrum was obtained at each pressure through the Ar medium using identical slit sizes and the absorbance was calculated at $-\ln(I/I_0)$, where I is the intensity of light transmitted though the sample, and I_0 is the intensity of light transmitted though the Ar. Some parasitic light transmission was observed for the $FASnBr_3$ sample due to the fine powder nature of the sample. This fact may contribute to the non-distinct absorption edges observed at several pressures.

Photoluminescence measurements

PL spectra were collected using a Princeton Instruments 2700 spectrograph with N_2 (liquid)-cooled Pylon CCD detector. A 405nm or 532 nm diode laser was focused onto the samples using a 20× LWD objective lens and attenuated to 2 mW (measured at the lens focal point). PL light was collected at 180 degrees from the excitation path and resolved spatially using confocal optics with a 50 μm pinhole. PL light was then focused onto the entrance slit (50 μm) of the spectrograph and dispersed

using a 300 groove/mm grating, then focused onto the detector. Spectra were normalized by the collection time.

X-ray Diffraction

High-pressure Powder diffraction data were collected on the ID15b beamline at the ESRF, Grenoble at incident radiation λ=0.4116 Å up to ~6 GPa and upon decompression. A Mar555 flat panel detector was placed at 400 mm distance from the sample. High pressure was obtained by loading a diamond anvil cell (DAC) using He as pressure transmitting medium. Pressure determination was done by ruby luminescence method, using the scale proposed by Mao *et al.*.[S7] Diffraction images were collected while rotating the cell by 64 degrees with 0.5 deg. step. Images were merged together and integrated into 1D pattern using Dioptas[S8] and lattice parameters were refined via LeBail method using the software GSAS and its graphical interface EXPGUI[S9].

References:

(S1) Gonzalez-Platas, J.; Alvaro, M., Nestola, F.; Angel, R. J. EosFit7-GUI: A new GUI tool for equation of state calculations, analyses and teaching. *Journal of Applied Crystallography 49*, 2016, 1377-1382.

(S2) Giannozzi, P.; Baroni, S.; Bonini, N.; Calandra, M.; Car, R.; Cavazzoni, C.; Ceresoli, D.; Chiarotti, G. L.; Cococcioni, M.; Dabo, I., et al. QUANTUM ESPRESSO: A Modular and OpenSource Software Project for Quantum Simulations of Materials. *J. Phys.: Condens. Matter* 2009, 21, 395502.

(S3) Perdew, J. P.; Burke, K. and Ernzerhof, M. Generalized gradient approximation made simple. *Phys. Rev. Lett*. 1996, 77, 3865–3868.

(S4) Heyd, J.; Scuseria, G. E.; Ernzerhof, M. Hybrid functionals based on a screened Coulomb potential. *J. Chem. Phys.* 2003, 118, 8207-8215.

(S5) Du, M.-H. Density Functional Calculations of Native Defects in $CH_3NH_3PbI_3$: Effects of Spin–Orbit Coupling and Self-Interaction Error. *J. Phys. Chem. Lett*. 2015, 6, 1461-1466.

(S6) Monkhorst, H. J.; Pack, J. D. Special points for Brillouin-zone integrations. Phys. Rev. B 1976, 13, 5188-5192.

(S7) Mao, H. K.; Xu, J.; Bell, P. M. Calibration of the ruby pressure gauge to 800 kbar under quasi-hydrostatic conditions, *Journal of Geophysical Research: Solid Earth*, 1986, 4673.

(S8) Prescher, C.; Prakapenka, V.B. DIOPTAS: a program for reduction of two-dimensional X-ray diffraction data and data exploration. *High Press. Res.* 2015 35:3, 223–230.

(S9) Toby, B. H. EXPGUI, a graphical user interface for GSAS, *J. Appl. Cryst.* 34, 210-213 (2001)